ELSEVIER

Superconductivity at 161 K in thorium hydride ThH_{10}: Synthesis and properties

Dmitry V. Semenok [1,*,†], Alexander G. Kvashnin [1,2,†], Anna G. Ivanova [3], Volodymyr Svitlyk [4], Vyacheslav Yu. Fominski [5], Andrey V. Sadakov [6], Oleg A. Sobolevskiy [6], Vladimir M. Pudalov [6], Ivan A. Troyan [3], Artem R. Oganov [1,2,7,*]

[1] Skolkovo Institute of Science and Technology, Skolkovo Innovation Center 121025, 3 Nobel Street, Moscow, Russia
[2] Moscow Institute of Physics and Technology, 141700, 9 Institutsky Lane, Dolgoprudny, Russia
[3] Shubnikov Institute of Crystallography, Federal Scientific Research Center Crystallography and Photonics, Russian Academy of Sciences, Moscow 119333, Russia
[4] ID27 High Pressure Beamline, ESRF, BP220, 38043 Grenoble, France
[5] National Research Nuclear University MEPhI (Moscow Engineering Physics Institute), Kashirskoe sh., 31, Moscow 115409, Russia
[6] P.N. Lebedev Physical Institute, Russian Academy of Sciences, 119991 Moscow, Russia
[7] International Center for Materials Discovery, Northwestern Polytechnical University, Xi'an 710072, China

Here we report targeted high-pressure synthesis of two novel high-T_C hydride superconductors, $P6_3/mmc$-ThH_9 and $Fm\bar{3}m$-ThH_{10}, with the experimental critical temperatures (T_C) of 146 K and 159–161 K and upper critical magnetic fields (μH_C) 38 and 45 Tesla at pressures 170–175 Gigapascals, respectively. Superconductivity was evidenced by the observation of zero resistance and a decrease of T_C under external magnetic field up to 16 Tesla. This is one of the highest critical temperatures that has been achieved experimentally in any compound, along with such materials as LaH_{10}, H_3S and $HgBa_2Ca_x$-Cu_2O_{6+z}. Our experiments show that *fcc*-ThH_{10} has stabilization pressure of 85 GPa, making this material unique among all known high-T_C metal polyhydrides. Two recently predicted Th-H compounds, $I4/mmm$-ThH_4 (>86 GPa) and $Cmc2_1$-ThH_6 (86–104 GPa), were also synthesized. Equations of state of obtained thorium polyhydrides were measured and found to be in excellent agreement with the theoretical calculations. New phases were examined theoretically and their electronic, phonon, and superconducting properties were calculated.

Keywords: Thorium hydrides; USPEX; High pressure; Superconductivity; X-ray diffraction

Introduction

Hydrogen is the first, simplest, and most common chemical element in the Universe. The transition of molecular hydrogen to the metallic atomic phase at high pressures was calculated for the first time in 1935 by Wigner and Huntington [1], with later estimations [2–4] showing that such metallization takes place only at very high pressures (450–550 GPa), which have not been technically achievable for a long time. In 2004, Ashcroft [5] proposed that atomic hydrogen-rich phases with properties similar to pure atomic metallic hydrogen might form at lower pressures when hydrogen is combined with other elements. Theoretical calculations [6–8] show that the stoichiometry (the amount of hydrogen in a compound) of metal hydrides stable at ambient conditions (e.g., Th_4H_{15} [9,10]) is not sufficient to produce the unique properties of metallic hydrogen,

* Corresponding authors.
E-mail addresses: Semenok, D.V. (Dmitrii.Semenok@skoltech.ru), Oganov, A.R. (A.Oganov@skoltech.ru).
† These authors contributed equally to this work.

 https://doi.org/10.1016/j.mattod.2019.10.005

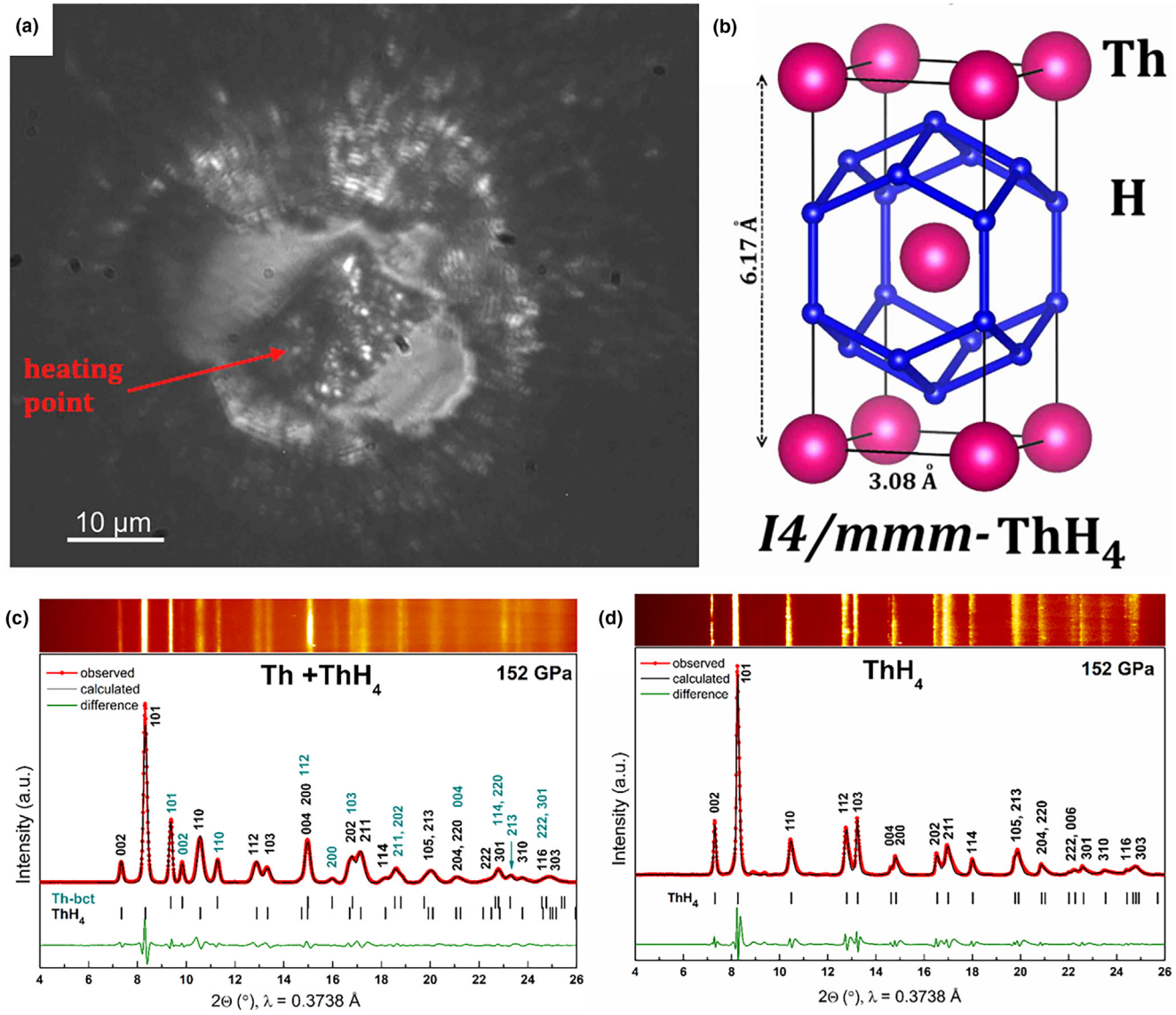

FIGURE 1

(a) Photograph of M2 sample after heating at 88 GPa. The heating point is shown by an arrow. (b) Crystal structure of *I*4/*mmm*-ThH_4 at 90 GPa. (c) Le Bail refinement for *bct*-Th and *I*4/*mmm*-ThH_4 after the second heating at 152 GPa; (d) Le Bail refinements of XRD pattern measured from the points where only *I*4/*mmm*-ThH_4 was observed at 152 GPa.

such as the high-T_C superconductivity [11]. New chemical compounds which possess excess of hydrogen and unexpected structures and stoichiometries, and can only be synthesized at high pressures, are required to reach the high-T_C superconductivity.

Room-temperature superconductivity has been an unattainable dream and subject of speculative discussions for a long time. However, the theoretical prediction of a high-temperature superconductor H_3S [12] followed by the experimental confirmation [13,14] has opened a new chapter in high-pressure physics - the study of superconducting hydrides. Recently predicted high-T_C superconducting hydrides of thorium [15], actinium [16], lanthanum, and yttrium [6], and experimental confirmation of record high-T_C superconductivity in LaH_{10} at 250–260 K [17,18] and successful synthesis of PH_3 [19,20] and previously predicted LaH_{10} [21], CeH_9 [22,23], UH_7, and UH_8 [24], YH_6 [25] motivated us to perform an experimental investigation of the Th-H system with a view to synthesize *fcc*-ThH_{10}, which was predicted to be a remarkable high-T_C superconductor [15]. According to our previous predictions, it should be stable at pressures above 80 GPa [15], the lowest known stabilization pressure among the high-T_C superconducting hydrides reported to date, and may have a T_C up to 241 K and critical magnetic field $H_C = 71$ T [15] at ~100 GPa, which makes the synthesis of this material very intriguing. Thus, the main goal of this study is the experimental synthesis of $Fm\bar{3}m$-ThH_{10} as a promising superconducting material [15]. The experimental high-temperature synthesis was performed by a short laser flash (200–500 ms) accompanied by the dissociation of ammonia borane, which leads to the generation of hydrogen with subsequent synthesis of higher hydrides as first demonstrated in the synthesis of LaH_{10} [17].

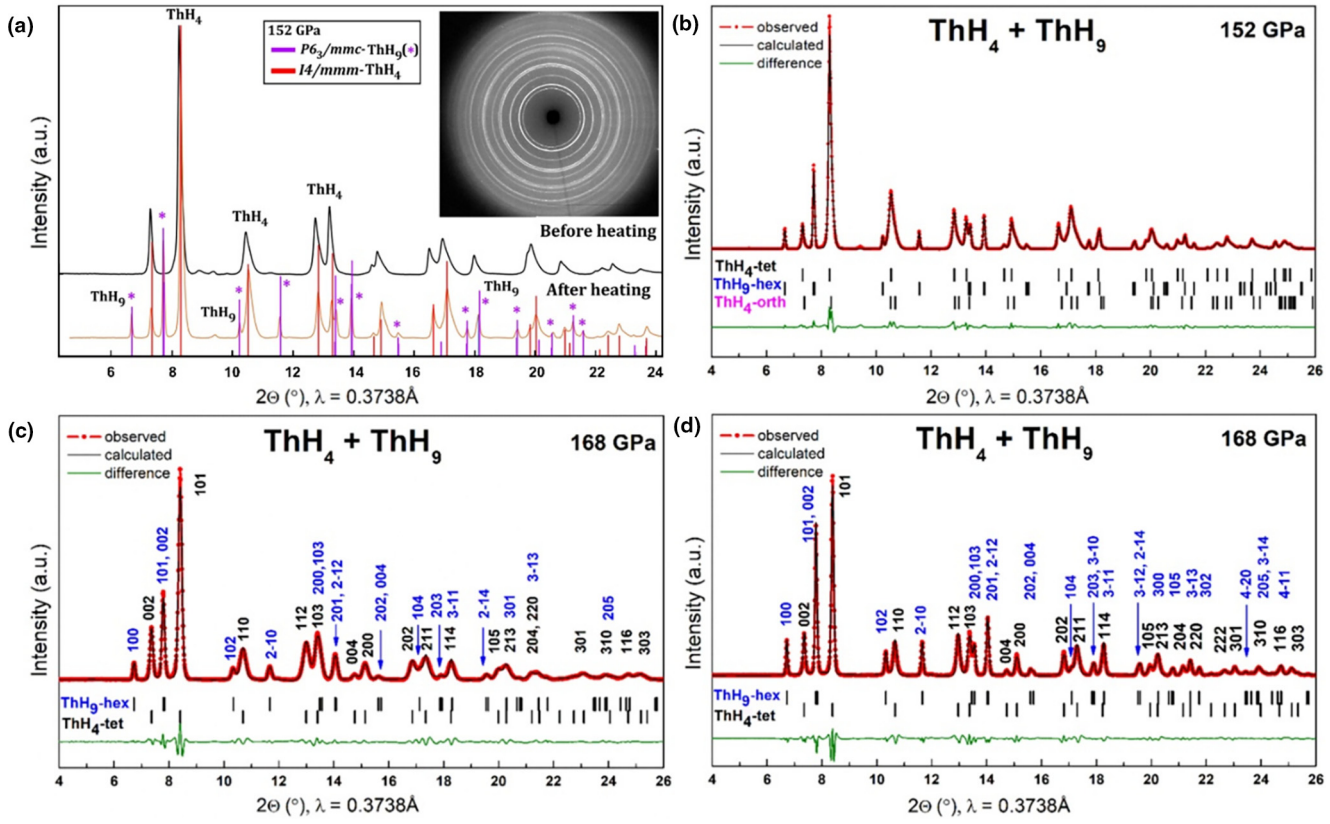

FIGURE 2

(a) Comparison of XRD patterns of M2 sample at 152 GPa before and after heating. The formation of ThH_9 is observed. New peaks are highlighted by the asterisks (*). The inset shows experimental XRD image obtained with the incident X-ray wavelength of 0.3738 Å; Le Bail refinements of $P6_3/mmc$-ThH_9 and ThH_4 at (b) 152 GPa and after the (c) third and (d) forth cycles of heating at 168 GPa (M2 sample). Red circles are experimental data; black line is the fit; green line shows residues.

Results and discussions

We prepared three samples, designated M1, M2, and M3. In this work we gradually increased the amount of hydrogen in the synthesized hydrides. In M2 sample, Th was loaded into a sublimated ammonia borane (AB) in the diamond anvil cell (DAC) and compressed to 98 GPa (see Table S2 in Supporting Information for details). The heating of M2 sample to 1800 K, performed at a single point by two 18 W laser pulses of 0.3 s, induces a pressure drop of 10 GPa which was measured by the Raman shift of diamond. The product was a mixture of *bct*-Th, *P*321-ThH_4, and *I*4/*mmm*-ThH_4 (Supporting Information Fig. S1). The two obtained tetrahydrides were predicted previously [15]. It is interesting to note that at the pressure of 100 GPa the hydrogen content in the compound increased just by 5% compared to *c*-Th_4H_{15}, which is stable at normal conditions.

Due to unsatisfactory results of the first heating, the applied pressure was increased to 152 GPa. A subsequent heating to ~1400 K by five laser pulses of 0.3 s with the power of 50 W led to the decrease in pressure to 148 GPa. The products were metallic thorium and *I*4/*mmm*-ThH_4, as seen from the X-ray diffraction pattern (Fig. 1c). Measurements taken at several points of the sample show only *I*4/*mmm*-ThH_4 (Fig. 1d), sometimes with X-ray reflections of *bcc*-W from the gasket (Supporting Information Fig. S3). During an additional heating of M2 sample, we synthesized a new compound, $P6_3/mmc$-ThH_9, which was predicted previously [15] as a metastable phase. We performed a comprehensive theoretical and experimental analysis of its stability and superconducting properties.

Synthesis of $P6_3/mmc$-ThH_9

One more step of laser heating of M2 sample was performed at 152 GPa by using four laser pulses of 0.3 seconds with the power of 60 W, which raised the temperature of M2 sample to ~2000 K at each flash. The XRD patterns of M2 sample after heating show the progressive formation of a new phase (Fig. 2a) at those points of the sample where only *I*4/*mmm*-ThH_4 was observed previously. New reflections were assigned to an unexpected hexagonal $P6_3/mmc$-ThH_9 phase, which forms during the $ThH_4 + 2.5H_2 \rightarrow ThH_9$ reaction. The details of its crystal structure and experimentally refined lattice parameters are shown in Supporting Information Tables S1 and S4, respectively. According to our predictions the thorium atoms here occupy the 2d Wyckoff position (1/3, 2/3, 3/4) in the hexagonal cell. The hydrogen atoms form an H_{28} cage around each Th atom with the Th-H distances from 2.11 Å to 2.18 Å. Simultaneously with the formation of this phase, the width and asymmetry of ThH_4 peaks increased, possibly related to the *I*4/*mmm* → *Fmmm*-ThH_4 phase transition (Fig. 2b, Fig. S28b in Supporting Information). This orthorhombic modification of ThH_4 is found to be isenthalpic with *I*4/

mmm-ThH_4 at this pressure, and to have a lower enthalpy at lower pressures.

To synthesize higher thorium hydrides, we increased the pressure in M2 sample to 168 GPa and heated it by two laser pulses of 0.5 s with the power of 65 W, which raised the temperature to 2100 K at each flash. After the heating, the pressure in the sample rose by ~4 GPa. The XRD patterns show the absence of any phases other than ThH_9 and ThH_4 (Fig. 2c). However, the ThH_4/ThH_9 ratio changed during the heating and the amount of ThH_9 went up (see Fig. 2d, Fig. S28 in Supporting Information). The samples with significant predominance of ThH_9 were obtained by applying a series of laser heatings. The weight fractions of the ThH_4 and ThH_9 phases in the mixture were calculated from the Rietveld refinement to be 40.8(4)% and 59.2 (7)% respectively (Fig. S18 in Supporting Information). ThH_9 was found to be isostructural with the previously predicted $P6_3/mmc$-UH_9 [24]. The shortest H-H distance in ThH_9 is smaller than that in UH_9 and equals 1.123 Å at 100 GPa and 1.099 Å at 150 GPa, compared to 1.144 Å at 100 GPa and 1.127 Å at 150 GPa for UH_9.

Our experiment with M2 sample showed that multiple laser heatings and higher pressure of the experiment lead to the formation of higher hydrides from the lower ones using NH_3BH_3 as a source of hydrogen. However, the first step of laser heating performed at the relatively low pressure of ~88 GPa precluded the synthesis of thorium superhydrides because of the formation of a mixture of lower hydrides, mainly *I4/mmm*-ThH_4. We also found that overheating the samples above 2200 K led to a destruction of the diamond anvil cell, while heating to lower than 1400 K was inefficient and resulted in mixtures of hydrides with a low H-content.

Stability and physical properties of $P6_3/mmc$-ThH_9

$P6_3/mmc$-ThH_9 was found to be a thermodynamically metastable phase in our previous calculations, therefore, we did not study its physical properties [15]. Having observed this phase experimentally, here we calculate its zero-point energy as $U_{ZPE}(V,T) = 1/2\int g(\omega(V))\hbar\omega d\omega$ and find that it leads to the stabilization of ThH_9 (Fig. 3a). Similar stabilization was found for the recently studied *C2/m*-Ca_2H_5 [26] and high-T_C superconducting LaH_{10} [17,18].

The crystal structure of $P6_3/mmc$-ThH_9 is similar to that of the previously predicted and synthesized CeH_9 [17] which can be explained by the similarity of electronic structures of Ce ($4f^15d^1$) and Th ($6d^2$) atoms. Zero-point energy plays a crucial role in stabilizing ThH_9 at pressures above 105 GPa (Fig. 3a). This lower limit of thermodynamic stability of ThH_9 is in excellent agreement with our experimental data. The study of the dynamical stability of ThH_9 at different pressures shows the absence of imaginary phonon frequencies at 100 GPa and 150 GPa (Fig. 3d

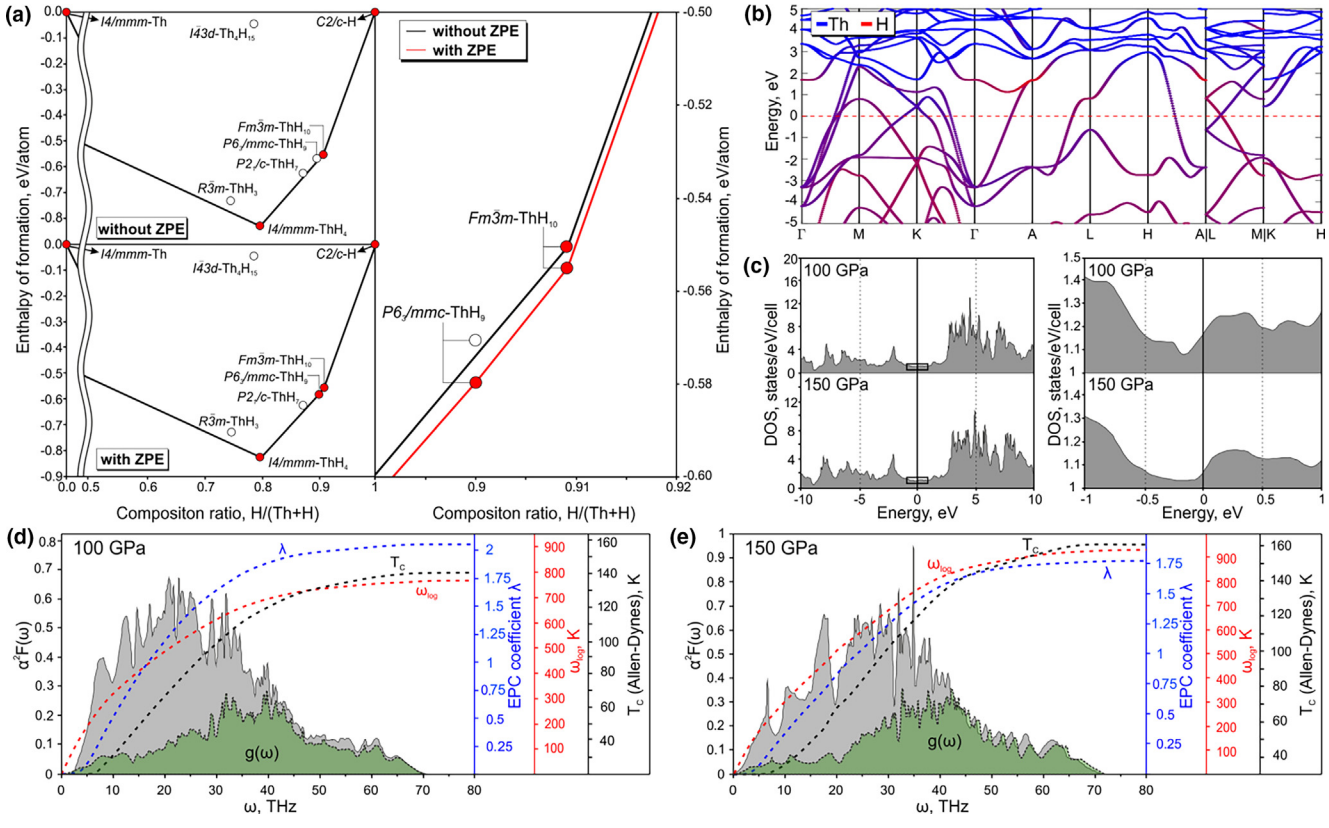

FIGURE 3

(a) (left) Thermodynamic convex hull of the Th-H system with and without the zero-point energy (ZPE) contribution at 150 GPa. (right) Magnified region near ThH_9 and ThH_{10} showing that ThH_9 is stabilized by the zero-point energy. (b) Band structure of $P6_3/mmc$-ThH_9 at 150 GPa. Contributions of hydrogen and thorium are shown in red and blue, respectively. (c) Electronic DOS of $P6_3/mmc$-ThH_9 at 100 GPa and 150 GPa shown energy ranges ±10 eV and ±1 eV around the Fermi level. (d) and (e) Phonon density of states (shown in green, in a.u.), Eliashberg $\alpha^2F(\omega)$ function (in black), and superconducting parameters of $P6_3/mmc$-ThH_9 at 100 GPa and 150 GPa.

and e and Supporting Information Fig. S21), which is consistent with our experiments. At pressures below 100 GPa, ThH_9 becomes dynamically unstable. Under the studied conditions, all thorium hydrides are metallic in both experiment and theory. The calculated band structure at 150 GPa shows the predominant contribution of hydrogen near the Fermi level (red color in Fig. 3b), which lies in an almost flat "valley" of the density of states.

We calculated the Eliashberg $\alpha^2F(\omega)$ function at 100 GPa and 150 GPa to find the critical temperature (T_C) and critical magnetic field (H_C), shown in Fig. 3d and e. At 150 GPa, ThH_9 has a high electron–phonon coupling (EPC) coefficient $\lambda = 1.73$ and a high logarithmic frequency $\omega_{log} = 957$ K, giving the predicted $T_C = 123$–145 K. Calculated superconducting parameters are summarized in Table 1.

We estimated the critical magnetic field and the jump in the specific heat for ThH_9 (see Table 1). The calculation of the upper critical magnetic field gives $\mu_0 H_C(0) \sim 39$ T at 150 GPa. The estimated coherence length $\xi_{BCS} = 0.5\sqrt{h/\pi eH_C}$ is 30 Å. The isotopic coefficient for $P6_3/mmc$-ThH_9 at 150 GPa is 0.48 using $\mu^* = 0.1$ in Allen–Dynes (A–D) formula (Table 1) in the harmonic approximation, and $T_C(ThD_9)$ is 89–104 K. T_C of ThH_9 slightly increases with pressure ($dT_C/dP = +0.06$–0.1 K/GPa), while for $Fm\bar{3}m$-ThH_{10}, the opposite dependence was predicted [15]. Extrapolation of these data to experimentally studied pressure point – 170 GPa leads to predicted interval of 125–147 K for T_C and 32–36 T for $\mu_0 H_C(0)$ which coincides well with the experiment (see Section 2.4).

Synthesis of $Fm\bar{3}m$-ThH_{10} and $Fm\bar{3}m \rightarrow Immm$ phase transition

ThH_{10} was predicted to be stable and have an extremely high T_C [15]. Here we used M3 sample (Supporting Information Table S2), with the increased initial pressure of 170 GPa, heating it to 1800 K by four laser pulses of 0.3 s each, which induced an increase in pressure to 183 GPa. Analysis of the measured X-ray diffraction pattern of the entire sample area showed that the sample consisted of only $Fm\bar{3}m$-ThH_{10} (Fig. 4a), theoretically predicted and studied earlier [15]. The XRD pattern also contained reflections from the tungsten gasket because of the relatively small size of the sample and chamber, ~20 μm. By the subsequent stepwise reduction of pressure in M3 sample from 183 GPa to 85 GPa (Fig. 4b), we measured the equation of state of $Fm\bar{3}m$-ThH_{10} (Fig. 6) and found the lower limit of stability of this phase. The experimental lattice parameters of this phase are shown in Table S5 (see Supporting Information). At a pressure close to the theoretically predicted lower limit of its stability (85 GPa [15]), we observed broadening and splitting of ThH_{10} XRD peaks accompanying the $Fm\bar{3}m \rightarrow Immm$-$ThH_{10}$ phase transition (see Supporting Information, Fig. S27). $Immm$-ThH_{10} ($a = 5.304(2)$ Å, $b = 3.287(1)$ Å, $c = 3.647(2)$ Å, $V = 74.03$ Å^3) is the closest in energy metastable modification of ThH_{10} that appears in experiments at pressures below 100 GPa. An additional signal observed at $2\theta = 7.455°$ was caused by the decomposition of ThH_{10} producing $P6_3/mmc$-ThH_9.

Cubic hydrogen-rich phase $Fm\bar{3}m$-ThH_{10} was the main goal of this study due to its predicted superconductivity with T_C up to 241 K [15] at 90–100 GPa. This is also in agreement with phonon

TABLE 1

Calculated parameters of the superconducting state of $P6_3/mmc$-ThH_9 at 100 GPa and 150 GPa using Allen–Dynes (A–D) formula. Here γ is the Sommerfeld constant, the values are given at μ^* equal to 0.15–0.1, β is the isotopic coefficient.

Parameter	$P6_3/mmc$-ThH_9	
	100 GPa	150 GPa
λ	2.15	1.73
ω_{log}, K	728	957
β	0.47–0.48	0.47–0.48
T_C (A–D), K	118–138	123–145
T_C ($P6_3/mmc$-ThD_9), K	85–99	89–104
$\Delta(0)$, meV	31.2–35.2	29.6–33.9
$\mu_0 H_C(0)$, T	37–41	33–37
$\Delta C/T_C$, mJ/mol·K^2	25.8	19.3–19.9
γ, mJ/mol·K^2	8.69	7.52
$R_\Delta = 2\Delta(0)/k_B T_C$	5.11–5.24	4.74–4.89

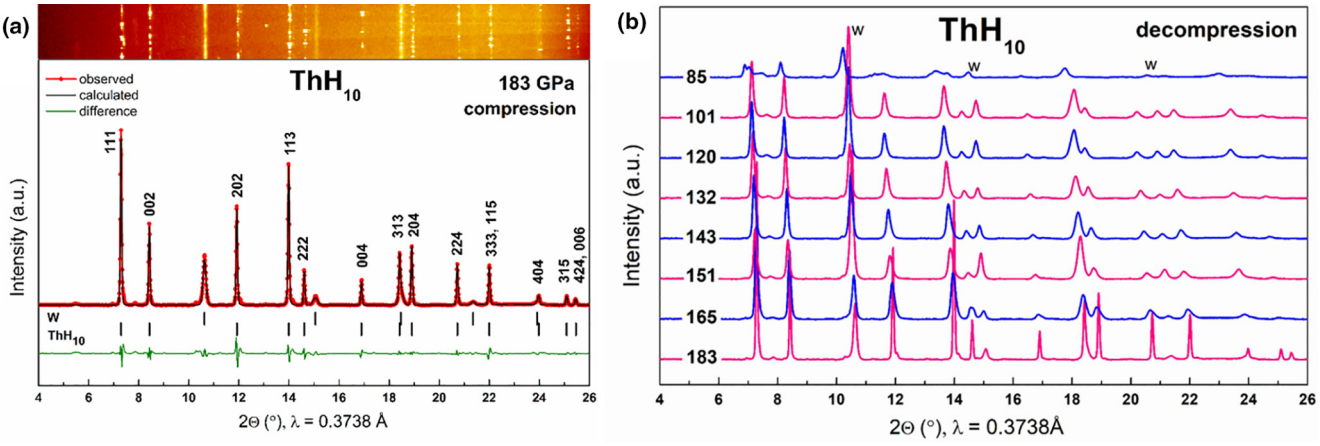

FIGURE 4

(a) Le Bail refinement of $Fm\bar{3}m$-ThH_{10} and *bcc*-W at 183 GPa. Experimental data are shown in red, fitted line and residues are shown as black and green lines, respectively. Rietveld refinement for ThH_{10} is given in Fig. S19 (Supporting Information). (b) Experimental XRD patterns of $Fm\bar{3}m$-ThH_{10} in the pressure range of 183–85 GPa.

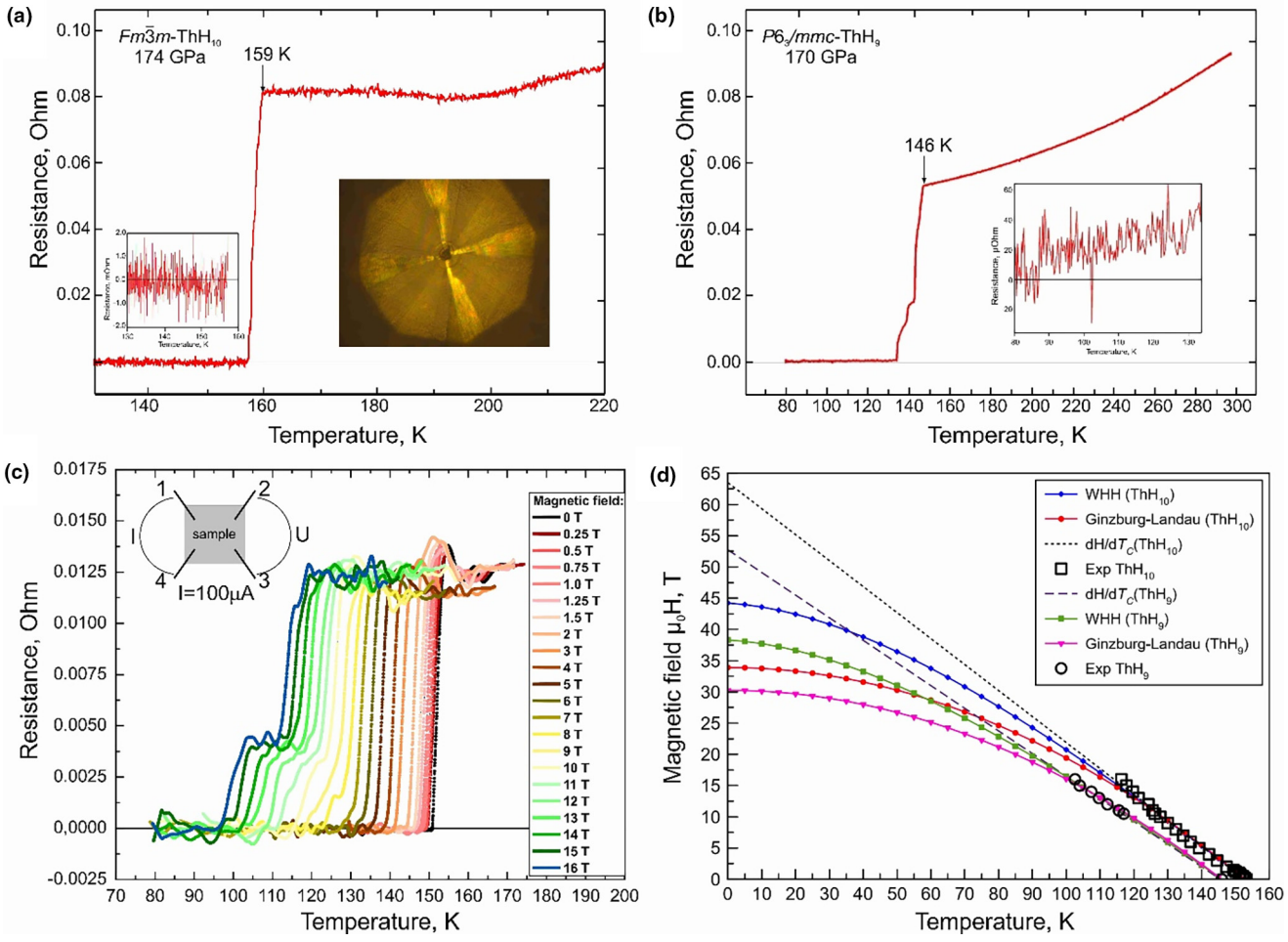

FIGURE 5

Observation of superconductivity in (a) ThH_{10} and (b) ThH_9. The temperature dependence of the resistance (R) of thorium superhydride was determined in a sample synthesized from Th + NH_3BH_3. The resistance was measured with four electrodes deposited on a diamond anvil on which the sample was placed (the right panel inset) at excitation current 100 μA. The resistance near the zero point is shown in a smaller scale in the insets; (c) dependence of resistance on temperature under external magnetic field at 170 GPa; (d) dependence of the critical temperature (T_C) of the ThH_{10} and ThH_9 on magnetic field.

calculations, which prove its dynamical stability down to ~85 GPa (Fig. S25 in Supporting Information). ThH_{10} is structurally similar to the already predicted cubic decahydrides ScH_{10} [27,28], YH_{10} [6], LaH_{10} [17,18,21], and AcH_{10} [16]. The shortest H–H distances in these materials form the sequence $d_{min}(AcH_{10}) < d_{min}(ThH_{10}) < d_{min}(LaH_{10})$ at 150 GPa (1.07 Å < 1.119 Å< 1.164 Å).

Measurements of superconducting properties of ThH_{10} and ThH_9

To measure the temperature of the transition of thorium hydride to the superconducting state, a cell which we denote M1 with diamond anvils and Ta/Au electrodes was prepared. We used the anvils with a 50 μm central culet beveled to 300 μm at 8.5°. Four Ta electrodes (~200 nm) with gold plating (~80 nm) were sputtered onto the piston diamond. We used a composite gasket consisting of a tungsten ring and MgO epoxy mixture insert for isolating the electrical leads.

A ~1 μm-thick thorium sample was sandwiched between the electrodes and AB in the gasket hole 20 μm in diameter. The pressure in the cell was increased to 179 GPa. Heating of the sample was performed by pulses of a Nd:YAG infrared laser with the wavelength $\lambda = 1.064$ μm, power of 35–40 W, and duration of 0.4 s. Raman spectra indicated the absence of the formation of any by-products (Fig. S29 in Supporting Information). The pressure in the chamber reduced to 174 GPa after laser heating (Fig. S30b in Supporting Information). The temperature dependence of the resistance is shown in Fig. 5. After the measurement, the cell was transferred to a synchrotron to confirm the structure of the hydride. The Le Bail refinement for the sample is shown in Fig. S31a (see Supporting Information).

We found that depending on the synthesis pressure, two different groups of superconducting transitions with T_C of 159–161 K (ThH_{10}, Figs. 5a and S31b in Supporting Information) and 146 K (ThH_9, Fig. 5b) can be observed, where the electrical resistance decreased sharply to zero (from 60 mΩ to 1–10 μΩ). The superconducting nature of the transitions was verified by their dependence on the external magnetic field in the range 0–16 Tesla. Fig. 5c shows that the applied magnetic field of $\mu_0 H = 4.1$ T reduces the onset of the superconducting transition by 10 K. Starting from 8 T a new resistance step appears, Fig. 5c. This step may be well explained by impurities of

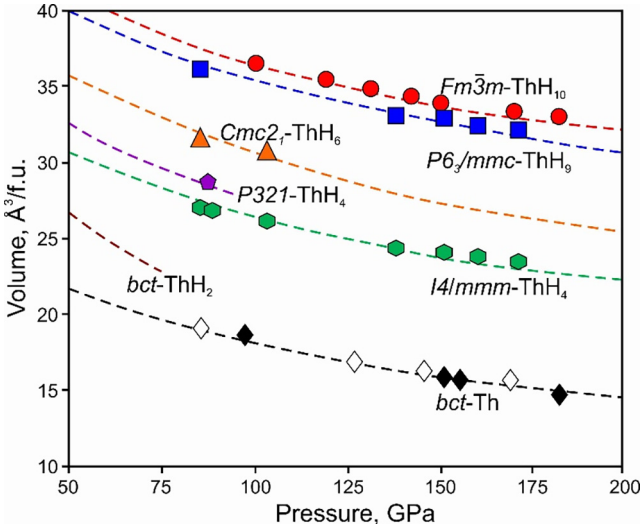

FIGURE 6

Equations of state of polyhydrides synthesized in this work in comparison with theoretical predictions and previously published data from Ref. [39].

hcp-ThH_9 (see Fig. S30a, Supporting Information) which has lower H_C and $|dH/dT_C| = 0.36$ T/K, and cannot be distinguished from the transition in *fcc*-ThH_{10} in weaker magnetic fields due to proximity-induced superconductivity [29].

Extrapolation of the temperature-dependent upper critical fields $\mu_0 H_{C2}(T)$ by linear function (dotted and dashed lines in Fig. 5d) yields about 64 and 53 T for *fcc*-ThH_{10} and *hcp*-ThH_9, respectively. The use of Werthamer–Helfand–Hohenberg (WHH) model [30] simplified by Baumgartner et al. [31] gives the values of 45 T (ThH_{10}) and 38 T (ThH_9) (Fig. 5d).

It is interesting to compare the experimentally obtained values with theoretical calculations based on the Bardeen–Cooper–Schrieffer and Migdal–Eliashberg theories. Superconductivity of thorium decahydride in the harmonic approximation was studied before [15] and the critical temperature was found to be in the range 150–183 K at 200 GPa (the Allen–Dynes formula [32], $\mu^* = 0.15$–0.1). Linear interpolation to 174 GPa gives T_C in the range 160–193 K (calculations done at 174 GPa give 167–183 K), in a good agreement with the measured value of 161 K. However, more rigorous theoretical values of Tc, obtained by solving Eliashberg equations, are significantly higher, 206–227 K.

Calculations of the electron–phonon interaction in cubic ThH_{10} at 174 GPa yield $\lambda = 1.75$, $\omega_{\log} = 1520$ K, and $\mu_0 H_{C2}(0) = 38$ T, the latter being slightly lower than experimentally found value (45 T, WHH model, Fig. 5d), but much lower than the Clogston–Chandrasekhar paramagnetic limit (when magnetostatic polarization energy exceeds Cooper pairs condensation energy) $\Delta_0/\sqrt{2}$ (359 T) [33]. Estimation of the average Fermi velocity $V_F \sim 4.12 \times 10^5$ m/s makes it possible to calculate the London penetration depth $\lambda_L \sim 136$ nm, coherence length $\xi_{BCS} = 29$ nm, and lower critical magnetic field $\mu_0 H_{C1} = 0.024$ T. The critical current density ($J_C = en_eV_L$), evaluated by Landau criterion for superfluidity [34] $V_L = min\frac{\varepsilon(p)}{p} \cong \frac{\Delta_0}{\hbar k_F}$, was calculated to be $\sim 3.16 \times 10^8$ A/cm^2, much higher than in H_3S [13]. The calculated Ginzburg–Landau parameter [35] is over 46, which is typical for II type superconductors.

Equations of state

By decompressing M2 sample from 168 GPa to 86 GPa and further down until its destruction (cracking, Supporting Information Fig. S4a), we studied the equation of state of *I*4/*mmm*-ThH_4 and *P*6$_3$/*mmc*-ThH_9 and obtained the previously predicted low-symmetry thorium hexahydride *Cmc*2$_1$-ThH_6 [15] (Supporting Information Fig. S4). Le Bail refinements of observed hydrides are shown in Figs. S7–S9 in Supporting Information. The experimental equations of state (Fig. 6) of the synthesized thorium hydrides are in close agreement with theoretical predictions [15].

Experiments of this study can be used to assess the predictive power of the evolutionary algorithm USPEX [36–38], which was used to predict thorium polyhydrides [15]. Here, we synthesized thorium decahydride ThH_{10} along with thorium hexa- and tetrahydrides (*Cmc*2$_1$-ThH_6, *P*321- and *I*4/*mmm*-ThH_4), which were predicted before [15]. Also, *hcp*-ThH_9, a new superconductor with T_C of 146 K, was synthesized. Thus, the experiment proves reliability of the USPEX predictions.

The example of the Th-H system, together with the Ce-H, U-H and La-H systems, shows that the lower bound of stability of metal polyhydrides shifts toward lower pressures when going down the Periodic Table. Increasing the complexity to ternary (A-B-H) systems might lead to further lowering of the synthesis pressure and further increase of T_C. Theory is set to play a leading role in the study of such systems.

Conclusions

The high-T_C superconductors *Fm*$\bar{3}$*m*-ThH_{10} and new *P*6$_3$/*mmc*-ThH_9, as well as three other previously predicted polyhydrides, *Cmc*2$_1$-ThH_6, *P*321-ThH_4, and *I*4/*mmm*-ThH_4 were synthesized, confirming earlier theoretical predictions [15]. Predicted lower bound of dynamical stability of ThH_{10} (80 GPa) is in excellent agreement with the experimentally determined value (~85 GPa), i.e., *fcc*-ThH_{10} has a unique combination of high superconducting T_C (159–161 K at 175 GPa) and critical magnetic field $\mu_0 H_C(0)$ of 45 Tesla, and the stability pressure, which is much lower than that of other high-T_C hydrides. The measured parameters of the superconducting state of *hcp*-ThH_9 include T_C of 146 K, the upper critical magnetic field $\mu_0 H_C(0)$ of 38 Tesla, and the superconducting gap of ~35 meV. In addition, we experimentally observed pressure-driven phase transitions in ThH_4 (*P*321 → *I*4/*mmm* → *Fmmm*) and ThH_{10} (*Fm*$\bar{3}$*m* → *Immm*). The rich observed chemistry of the Th-H system agrees with our theoretical predictions [15]. Stable and metastable phases predicted using the USPEX method can serve as a good guide for an experimental synthesis. The experiments performed will have a strong impact on our understanding of high-pressure chemistry of metal hydrides, bringing us closer to attaining room-temperature superconductivity at high and, hopefully, ambient pressures.

Methods

Experiment

To perform this experimental study, three diamond anvil cells (DACs) were loaded. The diameter of the working surface of diamond anvils was 280 microns, they were beveled at an angle of

8.5° to form a culet of 50 μm. The data on these DACs are shown in Supporting Information Table S2. X-ray diffraction patterns of all samples in diamond anvil cells were recorded at ID27 synchrotron beamline at the European Synchrotron Radiation Facility (Grenoble, France) with the use of a focused (1.7 × 2.3 μm) monochromatic X-ray beam of 33 eV ($\lambda = 0.3738$ Å) and a Perkin-Elmer area detector placed at a distance of 364.12 mm from the sample. The exposure time was 30–100 s. CeO_2 standard was used for the distance calibration. The X-ray diffraction data were analyzed and integrated using Dioptas software package (version 0.4) [40]. The full profile analysis of the diffraction patterns and the calculation of the unit cell parameters were performed in JANA2006 program [41] using the Le Bail method [42]. The heating of the samples was done by pulses of Nd:YAG infrared laser with the wavelength $\lambda = 1.064$ μm, power of 18–40 W, and duration of 300–500 ms. Temperature measurements were carried out using the decay curve of black body radiation within the Planck and Wien formulas at the laser heating system of ID27 beamline ESRF. The exact position of the heating spot was determined by an optical flash of a heated material detected by a CCD camera. The applied pressure was measured by the edge position of the Raman signal of diamond [43] using Acton SP2500 spectrometer with PIXIS:100 spectroscopic-format CCD. The pressure measurements were made using the Raman signals of a DAC. In the experimental X-ray images, the reflections from the BNH compounds are absent because of their amorphous state and weak X-ray scattering from light atoms.

Theory

The equations of state of the predicted ThH_4, ThH_6, ThH_9 and ThH_{10} phases were calculated using density functional theory (DFT) [44,45] within the generalized gradient approximation (Perdew–Burke–Ernzerhof functional) [46], and the projector-augmented wave method [47,48] as implemented in the VASP code [49–53]. Plane wave kinetic energy cutoff was set to 500 eV and the Brillouin zone was sampled using Γ-centered *k*-points meshes with resolution $2\pi \times 0.05$ Å^{-1}. Obtained dependences of the volume on pressure were fitted by the 3rd order Birch–Murnaghan equation [52] to determine the main parameters of the EOS, namely V_0, K_0 and K', where V_0 is the equilibrium volume, K_0 is the zero-pressure bulk modulus and $K_0^{'}$ its pressure derivative. Fitting was done using the EOSfit7 program [53]. We also calculated phonon densities of states of studied materials using the finite displacements method (VASP and PHONOPY [54,55]).

Calculations of superconducting T_C were carried out using QUANTUM ESPRESSO (QE) package [56]. Phonon frequencies and electron–phonon coupling (EPC) coefficients were computed using density-functional perturbation theory [57], employing plane-wave pseudopotential method and Perdew–Burke–Ernzerhof exchange–correlation functional [46]. In our *ab initio* calculations of the electron–phonon coupling (EPC) parameter λ, the first Brillouin zone was sampled using $4 \times 4 \times 4$ *q*-points mesh, and a denser $24 \times 24 \times 24$ *k*-points mesh (with Gaussian smearing and $\sigma = 0.025$ Ry, which approximates the zero-width limit in the calculation of λ). T_C was calculated from the Eliashberg equations [58] which were solved by iterative self-consistent method for the imaginary part of the order parameter $\Delta(T, \omega)$ (superconducting gap) and the renormalization wave function $Z(T, \omega)$ [59] (see Supporting Information). More approximate estimates of T_C were made using the Allen–Dynes formula [32].

Our calculations show that all found thorium hydrides are diamagnetic and are thermodynamically stable at conditions where experiments found them. As the new unexpected phase $P6_3/mmc$-ThH_9 has not been studied before, we performed additional calculations of its electronic, phonon and superconducting properties in the pressure range 100–200 GPa.

Author contributions

D.V.S., I.A.T, A.G.I. and V.Y.F. Performed the experiment. A.G.K. and A.R.O. prepared the theoretical analysis. D.V.S., A.G.K. and A.G.I. contributed to the interpretation of the results. D.V.S., A.G.K., A.R.O. wrote the manuscript. A.V.S., O.A.S. and V.M.P. performed magnetotransport experiments in high magnetic fields and participated in the data processing and discussions. All authors provided critical feedback and helped shape the research, analysis and manuscript.

Acknowledgments

Experiments were performed on were ESRF (Grenoble, France), station ID27. The authors express their gratitude to K. German (IGIC) and I. Polovov (URFU) for the technical assistance. I.A.T. and A.G.I. acknowledge the Ministry of Science and Higher Education of the Russian Federation within the State assignment of the FSRC "Crystallography and Photonics" of RAS in part of high pressure structural experiments and by the Russian Science Foundation (Project No.19-12-00414) in part of high pressure studies of superconductivity. A.G.K and D.V.S. thank the RFBR for the financial support of this work according to the project №19-03-00100. A.G.K. thanks the FACIE foundation UMNIK grant №13408GU/2018. A.R.O. thanks the Russian Science Foundation (grant 19-72-30043). A.V.S., O.A.S. and V.M.P. acknowledge support by the Program of the Presidium of RAS.

Appendix A. Supplementary data

Supplementary data to this article can be found online at https://doi.org/10.1016/j.mattod.2019.10.005.

References

[1] E. Wigner, H.B. Huntington, J. Chem. Phys. 3 (1935) 764–770.
[2] J.M. McMahon et al., Rev. Mod. Phys. 84 (2012) 1607–1653.
[3] S. Azadi et al., Phys. Rev. Lett. 112 (2014) 165501.
[4] J. McMinis et al., Phys. Rev. Lett. 114 (2015) 105305.
[5] N.W. Ashcroft, Phys. Rev. Lett. 92 (2004) 187002.
[6] H. Liu et al., PNAS 114 (2017) 6990–6995.
[7] F. Peng et al., Phys. Rev. Lett. 119 (2017) 107001–107007.
[8] H. Wang et al., Wiley Interdiscip. Rev.: Comput. Mol. Sci. 8 (2018) e1330.
[9] M. Dietrich et al., Solid State Commun. 15 (1974) 941–943.
[10] M.S. Wickleder, B. Fourest, P.K. Dorhout, in: The Chemistry of the Actinide and Transactinide Elements, Springer, Dordrecht, 2008, pp. 52–160.
[11] N.W. Ashcroft, Phys. Rev. Lett. 21 (1968) 1748–1749.
[12] D. Duan et al., Sci. Rep. 4 (2014) 6968.
[13] A.P. Drozdov et al., Nature 525 (2015) 73–76.
[14] I. Troyan et al., Science 351 (2016) 1303–1306.
[15] A.G. Kvashnin et al., ACS Appl. Mater. Interfaces 10 (2018) 43809–43816.
[16] D.V. Semenok et al., J. Phys. Chem. Lett. 9 (2018) 1920–1926.
[17] M. Somayazulu et al., Phys. Rev. Lett. 122 (2019) 027001.

[18] A.P. Drozdov et al., Nature 569 (2019) 528.
[19] A.P. Drozdov, M.I. Eremets, I.A. Troyan, ArXiv:1508.06224 (2015) http://arxiv.org/abs/1508.06224.
[20] H. Liu et al., J. Phys. Chem. C 120 (2016) 3458–3461.
[21] Z.M. Geballe et al., Angew. Chem. Int. Ed. 57 (2017) 688–692.
[22] N.P. Salke, et al., ArXiv:1805.02060 (2018) https://arxiv.org/ftp/arxiv/papers/1805/1805.02060.pdf.
[23] X. Li et al., Nat. Commun. 10 (2019) 1–7.
[24] I.A. Kruglov et al., Sci. Adv. 4 (2018) eaat9776.
[25] I.A. Troyan et al., ArXiv:1908.01534 [Cond-Mat] (2019).
[26] A.K. Mishra et al., J. Phys. Chem. C 122 (2018) 19370–19378.
[27] K. Abe, Phys. Rev. B 96 (2017) 144108.
[28] X. Ye et al., J. Phys. Chem. C 122 (2018) 6298–6309.
[29] R.D. Parks, Superconductivity: In Two Parts: Volume 2, 1st edition, Routledge, 2018.
[30] N.R. Werthamer, E. Helfand, P.C. Hohenberg, Phys. Rev. 147 (1966) 295–302.
[31] T. Baumgartner et al., Supercond. Sci. Technol. 27 (2013) 015005.
[32] P.B. Allen, R.C. Dynes, Phys. Rev. B 12 (1975) 905–922.
[33] A.M. Clogston, Phys. Rev. Lett. 9 (1962) 266–267.
[34] L. Landau, Phys. Rev. 60 (1941) 356–358.
[35] V.L. Ginzburg, L.D. Landau, Zh. Eksp. Teor. Fiz. 20 (1950) 1064–1082.
[36] A.R. Oganov, C.W. Glass, J. Chem. Phys. 124 (2006) 244704.
[37] A.R. Oganov et al., Rev. Mineral Geochem (2010) 271–298.
[38] A.R. Oganov, A.O. Lyakhov, M. Valle, Acc. Chem. Res. 44 (2011) 227–237.
[39] Y.K. Vohra, J. Akella, High Pressure Res. 10 (1992) 681–685.
[40] C. Prescher, V.B. Prakapenka, High Pressure Res. 35 (2015) 223–230.
[41] V. Petříček, M. Dušek, L. Palatinus, Z. Kristallogr. Crystall. Mater. 229 (2014) 345–352.
[42] A.L. Bail, Powder Diffr. 20 (2005) 316–326.
[43] Y. Akahama, H. Kawamura, J. Phys.: Conf. Ser. 215 (2010) 012195.
[44] P. Hohenberg, W. Kohn, Phys Rev 136 (1964) B864–B871.
[45] W. Kohn, L.J. Sham, Phys Rev 140 (1965) A1133–A1138.
[46] J.P. Perdew, K. Burke, M. Ernzerhof, Phys. Rev. Lett. 77 (1996) 3865–3868.
[47] P.E. Blöchl, Phys. Rev. B 50 (1994) 17953–17979.
[48] G. Kresse, D. Joubert, Phys. Rev. B 59 (1999) 1758–1775.
[49] G. Kresse, J. Furthmüller, Phys. Rev. B 54 (1996) 11169–11186.
[50] G. Kresse, J. Hafner, Phys. Rev. B 47 (1993) 558–561.
[51] G. Kresse, J. Hafner, Phys. Rev. B 49 (1994) 14251–14269.
[52] F. Birch, Phys. Rev. 71 (1947) 809–824.
[53] R.J. Angel, M. Alvaro, J. Gonzalez-Platas, Z. Kristallogr. Crystall. Mater. 229 (2014) 405–419.
[54] A. Togo, I. Tanaka, Scr. Mater. 108 (2015) 1–5.
[55] A. Togo, F. Oba, I. Tanaka, Phys. Rev. B 78 (2008) 134106.
[56] P. Giannozzi et al., J. Phys.: Condens. Matter 21 (2009) 395502.
[57] S. Baroni et al., Rev. Mod. Phys. 73 (2001) 515–562.
[58] G.M. Eliashberg, JETP 11 (1959) 696–702.
[59] P.B. Allen, R.C. Dynes, Technical Report #7 TCM/4/1974 (1974).